2581-4575

International Journal For Recent Developments in Science & Technology

Crossref

A Peer Reviewed Research Journal

DYNAMIC POWER IMPLEMENTATION OF PV PEM FUEL CELL BASED STANDALONE AC/DC MICROGRID USING HYBRID ENERGY STORAGE

[#1]G.S.BHANU SRI, [#2]D.RAMESH BABU

[1]M.TECH STUDENT, DEPARTMENT OF EEE, KAKINADA INSTITUTE OF TECHNOLOGICAL SCIENCES (KITS), RAMACHANDRAPURAM

[2]ASSISTANT PROFESSOR, DEPARTMENT OF EEE, KAKINADA INSTITUTE OF TECHNOLOGICAL SCIENCES (KITS), RAMACHANDRAPURAM.

Abstract – In this paper, dynamic power management scheme is proposed for standalone hybrid AC/DC microgrid which constitutes photovoltaic (PV) based renewable energy source, proton exchange membrane (PEM) fuel cell (FC) as a secondary power source and battery-super capacitor as hybrid energy storage. The power management algorithm accounts for seamless operation of microgrid under various modes and state of charge (SoC) limit conditions of hybrid energy storage, when all the sources, storages and loads are connected directly at the dc link. The power management scheme (PMS) generates current references for dc converter current controllers of fuel cell, battery and super capacitor. The average and fluctuating power components are separated using moving average filter. The dc link voltage regulation under dynamic changes in load and source power variation is proposed. Also, PV power curtailment through control is formulated. The proposed power management is modified and extended to multiple photovoltaic generation system and batteries with all the sources and storages geographically distributed operating under multi-time scale adaptive droop based control with supervisory control for mode transition. The proposed power management scheme is validated using simulation results. Also, FPGA/Labview based laboratory scale experimental results are presented to validate the power management scheme under various critical conditions.

Index Terms—PV, PEM fuel cell, power management, super capacitor, voltage source converter, standalone AC/DC microgrid, Moving average filter, Multi-time scale, droop.

1. INTRODUCTION

Microgrids, which consist of distributed power generation, energy storages and loads, are power network sub-systems that can be independently controlled [1], and can be operated in both grid-connected or island mode. Grid-connected microgrid is one of the key technologies to realize the potential benefits of distributed renewable generation. Lately, increasing attention has been paid to the research on DC microgrids. Compared to AC microgrids, DC microgrids are less complex, better integration with DC distributed RES and energy storage, and require fewer stages for power conversion. Due to these properties, DC microgrids are more efficient, secure and flexible [2-3]. Microgrids have the advantages to better integrate renewable energy to the main grid [4]. With the increased percentage of distributed renewable generations connected to the power network, the grid operation faces new challenges. For example, it has been reported that PV generation injecting an exceedingly distorted current into the grid [5]. The impacts of the increasing PV generation on the grid has been investigated, and based on the findings of various studies, several control techniques have been developed to reduce the disturbance to the grid, which include sliding mode control [6], Droop control [7], and feedback linearizing control [8].

International Journal For Recent Developments in Science & Technology
2581-4575
Crossref
A Peer Reviewed Research Journal

In each case, these control techniques are integrated with the battery charging/discharging controllers to absorb the PV fluctuation. Furthermore, a power management scheme (PMS) is proposed in [9] for two different hybrid ac/dc microgrids, and proposed a multi-time scale adaptive droop control strategy. It plays a key role in power regulation under different loads and PV fluctuations scenarios. In [10], a droop control is developed by means of advanced model predictive control (AMPC) for smart DC microgrid to enable a fast control due to the nature of this controller. In [11], a conventional PI controller was proposed for both battery and super capacitor controllers to absorb the fluctuating during PV power variation.

The above mentioned previous studies are mainly the implementation of various control strategies to regulate DC bus voltage in DC microgrids against load or PV fluctuations. These methods must has a full acknowledge of system parameters, but due to the system's non-linearity and variation, the relevant calculations are often complex. Compared to those techniques, the utilization of fuzzy logic controllers (FLCs) has been proposed as a way to deal with the non-linearity of the system, and at the same time, to absorb the fluctuations within the microgrid [12-18]. FLCs can efficiently handle non-linear systems, without the knowledge of the system parameters. Additionally, when fine-tuned, FLCs tend to outperform conventional controllers [19-20].

In this paper, two dynamic power management schemes are proposed for two different hybrid AC/DC microgrid configurations. The first configuration (MG1) consist of single PV and PEM fuel cell based hybrid power sources, single battery and supercapcitor based HES with dc loads and three phase inverter fed ac loads. Here, all the sources and HES are interfaced to dc link directly through their dc-dc converters, assuming they are at same geographical location, as presented in Fig. 1. The second configuration (MG2), consist of multiple PVs, single PEM FC, multiple batteries (BES) and single SC with dc and ac loads. Here, all the sources and storages are interfaced to dc link through cable connected at their individual dc-dc converters such that they are geographically distributed, as shown in Fig. 6.The proposed dynamic power management scheme (PMS) plays key role in dc link voltage regulation, current references generation and reference current tracking by current controller to drive dc-dc converters of PV, FC, SC and battery. The main contributions of the proposed dynamic power management scheme for MG1 and MG2 are

1. For MG1, current reference generation for PEM FC, Battery and SC using single dc link voltage controller.
2. For MG1, separation of average and transient current references using moving average filter (MAF).
3. For MG1, allocation of different current references to input current controllers of dc converters of PEM FC and HES by mode based power management algorithm to drive the system seamlessly from load dominating condition to generation dominating condition while maintaining power supply reliability even if the battery SoC and SC voltage are in limit condition.
4. The operation of PEM FC with effective utilization of H2 is also ensured. Also, control based de-rating operation of PV boost converter is presented.
5. For MG2, muti-time scale adaptive droop based control with input current controller to operate the DGs in distributed way is proposed. A novel MAF based droop is used for time-scaling of fast and slow DGs. The SoC based adaptive droop is proposed for operation of multiple BES.
6. For MG2, supervisory control based mode transition signal employing low bandwidth communication (LBC) is proposed to operate the

International Journal For Recent Developments in Science & Technology
2581-4575
Crossref
A Peer Reviewed Research Journal

sources/storages in droop mode/ MPPT Mode/ SoC control mode/ Voltage control mode.

2. System configuration

1. Hybrid AC/DC Microgrid Configuration 1

The hybrid AC/DC microgrid (MG1) configuration 1 consists of PV with boost converter and PEM fuel cell (FC) with boost converter, both interfaced directly at dc link, as shown in Fig. 1. It is supported by hybrid energy storage (HES) comprising battery and supercapacitor (SC) interfaced directly to dc link through bidirectional DC-DC converters (BDC). The load consists of dc load and three phase ac load fed by three phase voltage source converter (VSC). Fuel cell generates only steady state power to meet the excess power demand in case of very less/no PV power is available. The HES supports both the steady state as well as transient power changes in generation and loads. It also assists the fuel cell to slowly ramp up its generation from minimum/zero value to the reference value. The SC supports transient/fluctuating as well as oscillatory power changes and is insufficient to supply/absorb constant power changes (for long time duration) due to its low energy density. While battery support constant power changes due to its high energy density, it may also supply transient power (only under crucial circumstances). The VSC operates in voltage control mode with fixed frequency obtained from voltage controlled oscillator [1]-[2]. It supplies three phase ac load or three single phase ac loads. The PV power curtailment is obtained by operating it on the linear characteristic of PV curve between MPP (Vmp) point and open circuit (Voc). The modelling of PV connected to boost converter for MPP, Battery and SC connected to dc link through BDC and VSC control is discussed in detailed in [13].

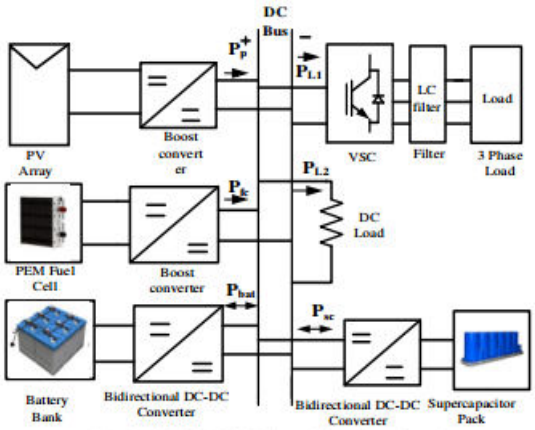

Fig. 1. Hybrid AC/DC Microgrid configuration 1

2. Hybrid AC/DC Microgrid Configuration 2

The hybrid AC/DC microgrid configuration 2 (MG2) consists of multiple PV sources with their individual boost converters, multiple battery bank with their individual bidirectional converters, a super capacitor pack with its bidirectional converter and a PEM fuel cell with its boost converters, connected to same dc link through cable having impedance mainly resistive at steady state. The dc loads and three phase inverter fed ac load are also connected at dc link, as presented in Fig. 2. Since, the sources and storages are geographically distributed hence, needs a modified power management scheme for reliable operation.

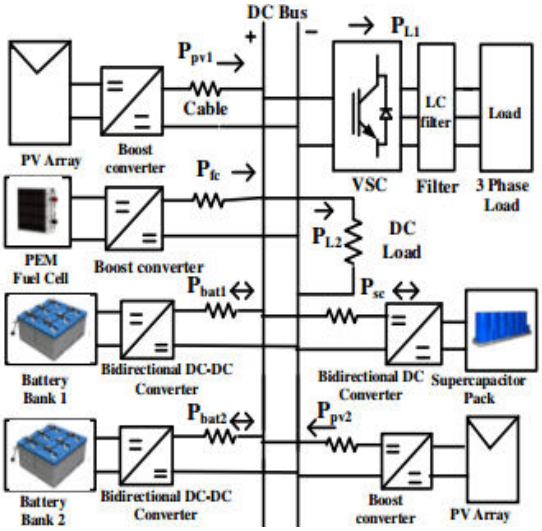

Fig. 2. Hybrid AC/DC Microgrid configuration 2

International Journal For Recent Developments in Science & Technology
2581-4575
Crossref
A Peer Reviewed Research Journal

3. Modelling and Control of PEM Fuel Cell

Some of the important relations that describes the modelling of PEM fuel cell are as follows [4]-[5]. Fuel cell stack current and hydrogen flow are related as

$$q_{h2}^{r} = N_0 I_{fc}/2F = 2K_r I_{fc} \quad (1)$$

Where , No is the number of series fuel cells in the stack, is stack current (A), F is faraday's constant (C/Kmol) and Kr is modeling constant (Kmol/(sA)-1).

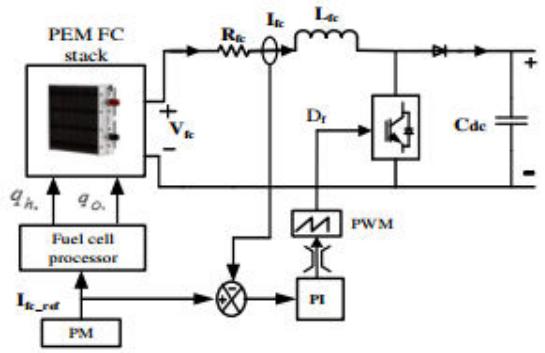

Fig. 3. PEM fuel cell with boost converter

The Polarization curve of the fuel cell gives the fuel cell voltage which is sum of the Nernst instantaneous voltage E, activation overvoltage and ohmic overvoltage and is expressed mathematically as follows.

$$V_{cell} = E + \eta_{act} + \eta_{ohmic} \quad (2)$$

Where, η_{act} is function of oxygen concentration Co_2 and I_{fc}, η_{ohmic} is function of I_{fc} and and stack internal resistance R^{int} (Ω). Assuming constant O_2 concentration and constant temperature, (2) can be written as

$$V_{cell} = E - B\ln(C\,I_{fc}) - R^{int} I_{fc} \quad (3)$$

Where, B=0.04777 V and C=0.0136 A^{-1}. The Nernst voltage in terms of gas molarities is given by [4]

$$E = N_0\left[E_0 + \frac{RT}{2F}\log\left[\frac{\rho_{h2}\,\rho_{O2}^{0.5}}{\rho_{H20}}\right]\right] \quad (4)$$

Where, E_0 is open cell voltage (V). Hydrogen utilization factor (U) is defined as the ratio of H_2 reacted inside the stack to the injected H_2 into the tank and has value between 0 and 1.

$$U = q_{h2}^{r} \Big/ q_{h2}^{in} \quad (5)$$

Values above 0.9 are indicative of over-utilization of hydrogen leading to fuel starvation and reduces its life and performance. On the other hand, values below 0.8 corresponds to underutilization of hydrogen which indicates the presence of excess hydrogen, leading to sharp rise in output voltage and reduction in overall power efficiency. Thus, for optimal utilization of H2 in fuel cell stack, stack current is limited by following criterion

$$\frac{0.8q_{h2}^{in}}{2K_r} \le I_{fc} \le \frac{0.9q_{h2}^{in}}{2K_r} \quad (6)$$

The current reference I_{fc_ref} obtained from the power management scheme generates the H_2 reference given by

$$q_{h2}^{ref} = \frac{2K_r I_{fc\_ref}}{U_{opt}} \quad (7)$$

In accordance to (6), the ramp rate of fuel cell reference current is controlled by current slope limiter (Ampere/sec) whose slope is based on current and power rating of PEM fuel cell [8]. Hence fuel cell avoids steep changes in load demands and guarantees matching the reactant delivery rate and the usage rate [9].

The PEM FC interfaced to dc link through boost converters operating in current mode control is shown in Fig.3. A conventional PI controller is implemented to track the reference current signal obtained from power management scheme and generates duty ratio to boost the fuel cell voltage to reference dc link voltage. The transfer function of fuel cell boost inductor current to converter duty ratio is given by [8],

$$\frac{\hat{\imath}_{FC}(s)}{\hat{d}_f(s)} = \frac{\frac{I_{FC}}{(1-D_f)}\left(1 + \frac{V_{dc}C_{dc}s}{(1-D_f)}\right)}{s^2 L_{FC}C_{dc} + sR_{FC}C_{dc} + (1-D_f)^2} \quad (8)$$

Where, LFC, RFC, and IFC are the inductance, resistance and current of boost converter inductor respectively, DF is converter duty ratio, N QRH %N are dc link voltage and capacitance respectively. The transfer function (8) is compensated using proportional integral (PI) controller to obtain stable compensated system as well as ensure zero or very less steady state

International Journal For Recent Developments in Science & Technology
2581-4575
Crossref
A Peer Reviewed Research Journal

tracking error. The compensated loop gain is stable with phase margin of 700 and bandwidth around 2500 Hz, as shown in Fig.4.

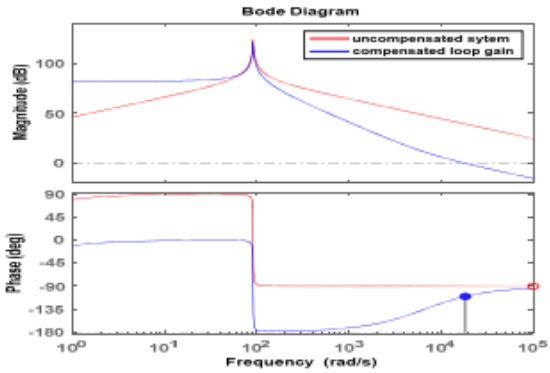

Fig.4. Bode plot of compensated loop gain and uncompensated loop gain

3.Control Strategy

3.1Control of Fuel Cell Subsystem

The fuel cell reference power is generated as the difference between the load power demanded minus the PV power. An additional power proportional to the difference of battery reference voltage and the current battery voltage is generated by an outer loop voltage controller to charge the battery. This additional power is then added to the fuel cell reference power demanded from the load to generate the overall fuel cell power reference. A proportional controller is sufficient for batteries with flat voltage profiles as in Li-ion battery. Fig. 5 shows the control strategy of the fuel cell subsystem.

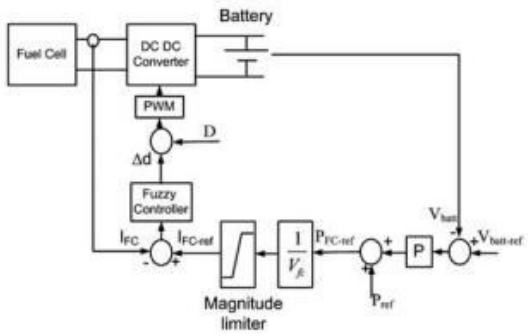

Fig. 5 Control of fuel cell subsystem.

In order to design control strategy for fuel cell power plant, two parameters should be considered and regulated. These parameters are hydrogen flow according to output power and fuel cell current. To control hydrogen flow from the fuel cell, a feedback from the stack current is considered that the reacting fuel quantity, 2 r H q , is directly proportional to the output current, Ifc, the factor Kr being a cell constant. Hence, the desired utilization is translated to corresponding output current demand:

$$q_{H_2}^{m} = \frac{2K_r}{U_{f,opt}} I_{demand}$$

A Proportional Integral (PI) controller is used to control the flow rate methane in the reformer. Oxygen flow is determined using the hydrogen-oxygen flow ratio rH-O. In the proposed control structure, choosing the control system parameters affects the system performance. So it is important to design PI controller properly. Another important parameter that must be controlled properly is fuel cell current. For this purpose, a boost DC-DC converter is selected for fuel cell converter. The current mode control of DC-DC converter has been used to regulate the fuel cell current. A typical range of Uf is 80-90% [4], which ensures that the operational limits mentioned above are observed. The corresponding limitation for the demand current is then calculated as following equation

$$\frac{0.8q_{H_2}^{m}}{2K_r} \equiv I_{k\_min} \le I_{k\_ref} \le I_{k\_max} \equiv \frac{0.9q_{H_2}^{m}}{2K_r}$$

To obtain transfer function of fuel cell current loop and apply classical control analysis and design methods (such as Nyquist criterion, Bode plots) in converter controls, the following transfer function can be investigated based on the state space signal models of boos DC-DC converter model [3, 16]:

$$T_{i_{FC}d}(s) = \frac{i_{FC}(s)}{d(s)} = \frac{1}{s^2 + \frac{R_L}{L}s + \frac{(1-D)^2}{LC}}\left[s\left(\frac{V_{C0}}{L}\right) + \frac{I_{L0}(1-D)}{LC}\right]$$

Moreover, the transfer function of PWM block can be modeled as:

International Journal For Recent Developments in Science & Technology
2581-4575
Crossref
A Peer Reviewed Research Journal

$$T_{PWM} = \frac{1}{K_{PWM}}$$

3.2Control of Grid Connected Voltage Source Converter

Control of grid connected voltage source converter is an important problem during voltage disturbances. It needs fast current controllers to track the current references according to change in active and reactive power during the fault. The current controller used in this paper consists of two vector current controllers based on Sliding Mode Control (SMC) that regulate the positive and negative sequence currents separately and are implemented in two different rotating coordinate systems. The need for regulating the positive and negative sequence currents is related for treating the unbalance voltage conditions.

A simplified scheme for the proposed control strategy is shown in Fig.6. The three phase grid currents and voltages are sampled and transformed into its positive and negative sequence components. The positive and negative sequence of dq-components are then used along the with the reference current signals to produce the reference voltage signals for the PWM regulator. A Sequence Separation Method (SSM) is needed to extract positive and negative sequences. Delayed Signal Cancellation method (DSC) is probably the best suited SSM [10]; but produces transient oscillations at the start and end period of voltage sag [5]. The abc system is first transformed into stationary αβ reference frame using Clark's transformation, and then it is delayed for T/4. The positive and negative sequences can be calculated by adding or subtracting the present real-time signal with delayed signal in the following way:

$$\begin{pmatrix} v_\alpha^p(t) \\ v_\beta^p(t) \\ v_\alpha^n(t) \\ v_\beta^n(t) \end{pmatrix} = \frac{1}{2}\begin{bmatrix} 1 & 0 & 0 & -1 \\ 0 & 1 & 1 & 0 \\ 1 & 0 & 0 & 1 \\ 0 & 1 & -1 & 0 \end{bmatrix}\begin{pmatrix} v_\alpha(t) \\ v_\beta(t) \\ v_\alpha(t-\frac{T}{4}) \\ v_\beta(t-\frac{T}{4}) \end{pmatrix}$$

According to the proposed control strategy, the purpose of the current controller is to synthesize a voltage correction vector so that the current error vector can be kept to a minimum value.

In this paper, the current controller has been implemented by using SMC technique due to its robustness and overshoot-free fast tracking capability .

The SMC is a nonlinear control approach which complies with the nonlinear characteristic of a power electronic converter. Such control technique is robust even against the plant parametric variation and can compensate the modeling approximations. Also, it is characterized by a good dynamic response. In addition, the SMC is simple to implement.

According to the dynamic model of inverter given, the state space equations of the system.

$$\dot{X}(t) = AX(t) + BU + EV_g$$
$$Y(t) = CX(t)$$

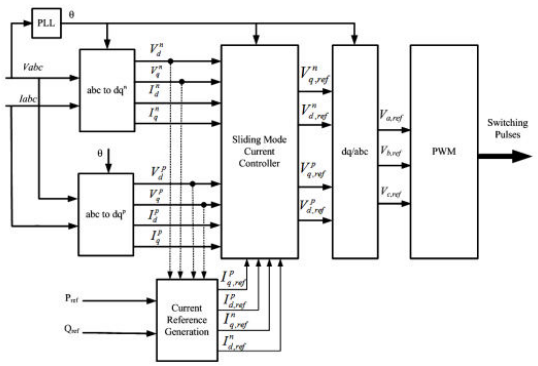

Fig.5 Block diagram of current control strategy

where the state variable is X, the control input U and grid voltage Vg

International Journal For Recent Developments in Science & Technology
2581-4575
Crossref
A Peer Reviewed Research Journal

$$X = \left[i_{2d}^{p} \;\; i_{2q}^{p} \;\; i_{2d}^{n} \;\; i_{2q}^{n} \right]^{T}$$

$$U = \left[U_{d}^{p} \;\; U_{q}^{p} \;\; U_{d}^{n} \;\; U_{q}^{n} \right]^{T}$$

$$V_{g} = \left[V_{gd}^{p} \;\; V_{gq}^{p} \;\; V_{gd}^{n} \;\; V_{gq}^{n} \right]^{T}$$

For the control plant given in Eq. (38), the sliding mode control law can be derived as follows. To let the current output Y track the reference input iref, a sliding mode manifold can be chosen

$$\begin{bmatrix} S_{p}^{dq} \\ S_{n}^{dq} \end{bmatrix} = \begin{bmatrix} i_{2dq}^{p} \\ i_{2dq}^{n} \end{bmatrix} - \begin{bmatrix} i_{2dq}^{p,ref} \\ i_{2dq}^{n,ref} \end{bmatrix}$$

where , 2 p ref dq i and , 2 n ref dq i are the specified current vector commands for the positive and negative sequence of dq components. The sliding mode can be reached if the control input U(t) is designed to be the solution

$$\frac{d}{dt} S(t) = 0$$

The control law satisfies is called equivalent control.

$$U_{eq}(t) = (CB)^{-1}[i_{ref} - CAX(t) - CEV_{g}(t)]$$

In order to generate proper current references, consider the complex apparent power from the grid:

$$S_{g} = (v_{sdq}^{p} e^{j\omega t} + v_{sdq}^{n} e^{-j\omega t}).(i_{2dq}^{p} e^{j\omega t} + i_{2dq}^{n} e^{-j\omega t})^{*} =$$
$$(P + P_{2c}.\cos(2\omega t) + P_{2s}.\sin(2\omega t)) +$$
$$j(Q + Q_{2c}.\cos(2\omega t) + Q_{2s}.\sin(2\omega t))$$

By expanding Eq., the following expression in matrix form can be written

$$P = (v_{sd}^{p}.i_{2d}^{p} + v_{sq}^{p}.i_{2q}^{p} + v_{sd}^{n}.i_{2d}^{n} + v_{sq}^{n}.i_{2q}^{n})$$
$$Q = (v_{sq}^{p}.i_{2d}^{p} - v_{sd}^{p}.i_{2q}^{p} + v_{sq}^{n}.i_{2d}^{n} - v_{sd}^{n}.i_{2q}^{n})$$
$$P_{c2} = (v_{sd}^{p}.i_{2d}^{n} + v_{sq}^{p}.i_{2q}^{n} + v_{sd}^{n}.i_{2d}^{p} + v_{sq}^{n}.i_{2q}^{p})$$
$$P_{s2} = (v_{sd}^{p}.i_{2q}^{n} - v_{sq}^{p}.i_{2d}^{n} - v_{sd}^{n}.i_{2q}^{p} + v_{sq}^{n}.i_{2d}^{p})$$
$$Q_{c2} = (v_{sq}^{p}.i_{2d}^{n} - v_{sd}^{p}.i_{2q}^{n} - v_{sd}^{n}.i_{2q}^{p} + v_{sq}^{n}.i_{2d}^{p})$$
$$Q_{s2} = (v_{sd}^{p}.i_{2d}^{n} + v_{sq}^{p}.i_{2q}^{n} - v_{sd}^{n}.i_{2d}^{p} - v_{sq}^{n}.i_{2q}^{p})$$

where P and Q are the constant active and reactive power, respectively, while the subscripts Ps2 and Pc2 represent the second harmonic sine and cosine component of the active power. These are the oscillating active powers due to the unbalance in the grid voltages. During generating the reference currents, the oscillating reactive powers (Q2c, Q2s) cannot be included in the calculation. Therefore to simplify the calculation and work with an invertible matrix (4×4), oscillating reactive power is not controlled and will flow through the system. Hence, the reference currents can be calculated as follow:

$$\begin{bmatrix} i_{2d}^{p*} \\ i_{2q}^{p*} \\ i_{2d}^{n*} \\ i_{2q}^{n*} \end{bmatrix} = \begin{bmatrix} v_{sd}^{p} & v_{sq}^{p} & v_{sd}^{n} & v_{sq}^{n} \\ v_{sq}^{p} & -v_{sd}^{p} & v_{sq}^{n} & -v_{sd}^{n} \\ v_{sq}^{n} & -v_{sd}^{n} & -v_{sq}^{p} & v_{sd}^{n} \\ v_{sd}^{n} & v_{sq}^{n} & v_{sd}^{p} & v_{sq}^{p} \end{bmatrix}^{-1} \begin{bmatrix} P^{*} \\ Q^{*} \\ -\Delta P_{s2} \\ -\Delta P_{c2} \end{bmatrix}$$

$$\Delta P = 2 \times (R_{1} + R_{2}) \times ((i_{2d}^{p})^{2} + (i_{2q}^{p})^{2} + (i_{2d}^{n})^{2} + (i_{2q}^{n})^{2})$$

$$\Delta P_{c2} = 2 \times (R_{1} + R_{2}) \times (i_{2d}^{p}.i_{2d}^{n} + i_{2q}^{p}.i_{2q}^{n}) +$$
$$2 \times \omega \times L \times (i_{2d}^{p}.i_{2q}^{n} - i_{2q}^{p}.i_{2d}^{n})$$

$$\Delta P_{s2} = 2 \times (R_{1} + R_{2}) \times (i_{2d}^{p}.i_{2q}^{n} - i_{2q}^{p}.i_{2d}^{n}) +$$
$$2 \times \omega \times (L_{1} + L_{2}) \times (-i_{2d}^{p}.i_{2d}^{n} - i_{2q}^{p}.i_{2q}^{n})$$

This algorithm calculates current references by setting active and reactive power references (P* , Q*), and by forcing the oscillating active power demanded by the filter to be delivered from the grid (* P2 2 c c = −ΔP ; * P2 2 s = −ΔP s). Then, no oscillating active power flows between the dc link and the filter.

The Phase Locked Loop (PLL) estimates the grid voltage phase angle which is then used to synchronize the inverter output voltage to the grid.

4. Simulation Studies

A. Simulation Results 1

The hybrid AC/DC microgrid configuration 1 is simulated under various modes and conditions discussed above to validate the proposed dynamic power management scheme 1 under dynamic load and source power variation. All the components

International Journal For Recent Developments in Science & Technology
2581-4575
Crossref
A Peer Reviewed Research Journal

are modelled in Matlab/Simulink in sim power system domain and parameters used for simulation are presented in Appendix.

1). Scenario I:

During t=0 to t=4 s, the system is working in Mode II, Condition F as the PV power is less than load power, as shown in Fig.6. The deficit power is supplied by fuel cell, battery and SC. At t= 2 s, PV power changes from 6.4 kW to 7.4 kW while at t= 4 s, load power decreases from 7.6 kW to 5.5 kW. Now, the hybrid microgrid operates in Mode I Condition A. Consequently, FC power start decreasing while SC and battery absorb power to maintain dc link voltage, as illustrated in Fig. 7 and Fig. 8. The battery absorbs the average power while SC compensates the oscillatory and transient power, as shown in Fig. 7. At t=7 s, battery SoC reaches its maximum value SoCBH (80%), hence system experiences critical Condition B and is presented in Fig.8. As a result, the power management scheme generates current references based on and executes PV de-rating loop to match load and PV power, as shown in Fig. 9. At t=8 s, the load power decreases to 4.6 kW. Again, PV de-rating loop decreases the PV boost converter duty ratio to force the SC current zero, as shown in Fig. 7 and Fig. 9. At this instant, SC supplies/absorbs a very small oscillatory power. At t =11.45 s, SC voltage reaches its maximum value VSCH, hence system enters into Mode I Condition D, as shown in Fig 10. Now, the dc link voltage is controlled to de-rate the PV power such that it power matches the load power, as presented in Fig. 11. At this instant, SC, battery and FC supply zero powers. Three phase line to line voltage of VSC output (380 V rms) and load current is shown in Fig. 12.

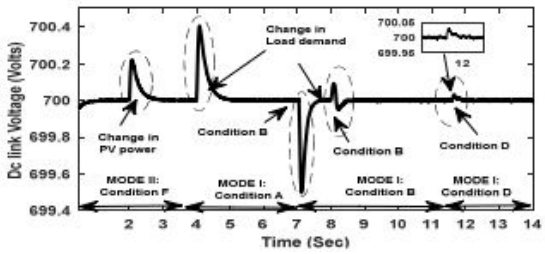

Fig. 6. Variation of dc link voltage scenario I

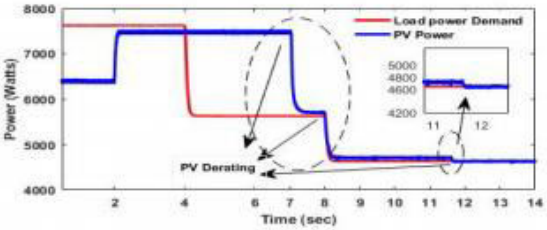

Fig.7. Variation of PV power and load power

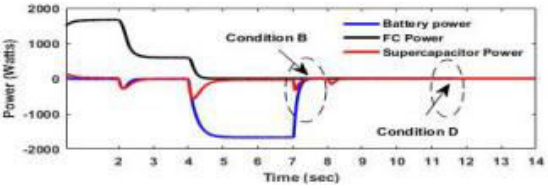

Fig.8. Variation of Battery, SC and FC powers scenario I

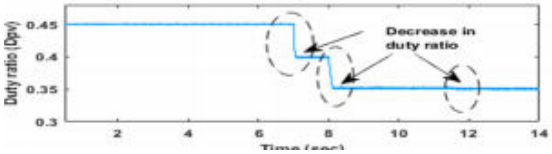

Fig.9. Variation of PV boost converter duty ratio scenario I

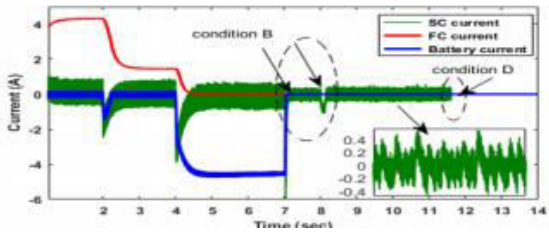

Fig.10. Variation of SC, FC and battery currents scenario I

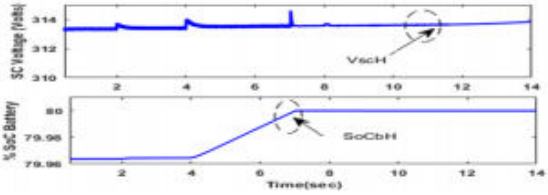

International Journal For Recent Developments in Science & Technology
2581-4575
Crossref
A Peer Reviewed Research Journal

Fig.11. Variation of SC voltage and % SoC of Battery scenario I

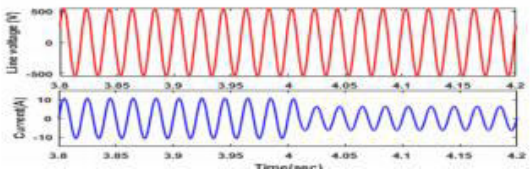

Fig. 12. Load voltage (L-L) and load current scenario I

2). Scenario II:

In this scenario, load dominating mode conditions are simulated. At t=2 s, PV power reduces from 5.5 kW to 4.5 kW and at t=4 s, again reduces to 3.4 kW, as shown in Fig.13 and Fig. 14. During t=0 to t= 6 s, load power of 6.4 kW is more than PV power hence the system operates in Condition F. The average deficit power is supplied by the FC assisted by battery and transient/oscillatory power being supplied by SC and is shown in Fig. 14. At t=6.1 s, battery reaches its lower SoC limit SoCBL (20%), as presented in Fig.15. Now, the power management algorithm produces current as system experiences Condition G. At t=9.94 s, the SC voltage reaches its lower voltage limit VSCL, therefore system experiences Condition I. Thus, PM produces zero current references for battery and SC while average current reference is supplied by FC and the converter current controller track these references effectively, -as presented in Fig. 15 and Fig.16 . The dc link voltage and input current controllers maintains the dc link almost constant at 700V reference even when subjected to step change in load and source powers, as shown in Fig. 6 and Fig. 8.

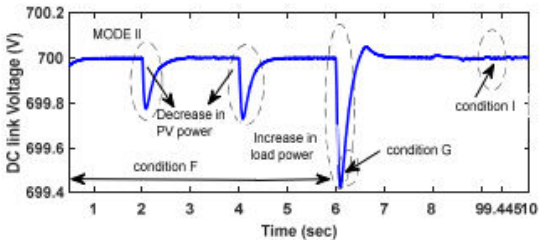

Fig. 13. DC link voltage variation scenario II

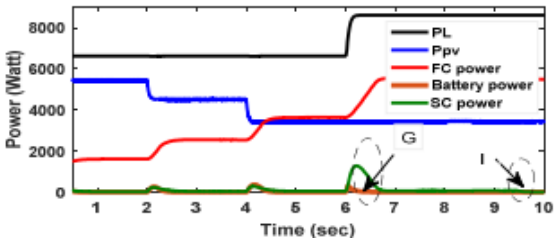

Fig. 14. PV, SC, FC, battery and load power scenario II

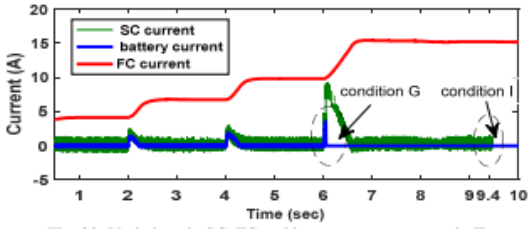

Fig. 15. Variations in SC, FC and battery currents scenario II.

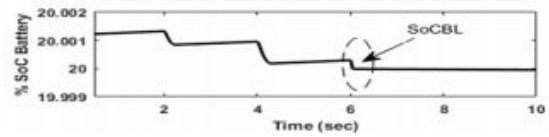

Fig. 16. Variations in % SoC of battery scenario II.

B. Simulation Results 2

The PMS proposed in Section V is validated for MG 2, presented in Fig.2. Initially MG2 is operating in generation dominating MODE I, Condition A. The load power changes from 8.73 kW to 6.57 kW at t=3 s and again decreases to 4.35 kW at t=5 s. The power supplied by PV1 and PV2 are 6.62 kW and 4.52 kW respectively, presented in Fig.18. The BES1 of 20 Ahr with 79.8% SoC and BES 2 of 10 Ahr with 79.85% SoC, absorbs power based on adaptive droop (31). The power absorbed by BES 2 changes from 0.74 kW to 1.45 kW at t=3 s, and to 2.17 kW at t=5s, and hits its SoCBH at 7.5 s, thus MG2 enters in Condition C. The BES 1 absorbed power changes - from 1.5 kW to 2.9 kW at t=3 s, to 4.35 kW at 5 s and 6.5 kW at 7.5 s and hits it's SoCBH at 8.75 s, shown in Fig. 20 and Fig. 21. Hence, the MG2 enters in Condition D, so the PVs changes its operation from MPPT mode to droop mode and shares same power of 2.27 kW, presented in Fig.

International Journal For Recent Developments in Science & Technology
2581-4575
Crossref
A Peer Reviewed Research Journal

18. The SC supplies transient power while BES shares average power based on multi-time scale droop. The PEM FC supplies zero power. The dc link voltage rises from 700 V to 703.5 V till 7.5 s while decreases to 699.3 V at 8.75 s, as shown in Fig. 17. Thus, the presented PMS for MG2 is robust to mode transitions without any oscillations due to use of MAF based multi-time scale adaptive droop constant as compared to LPF based droop constant.

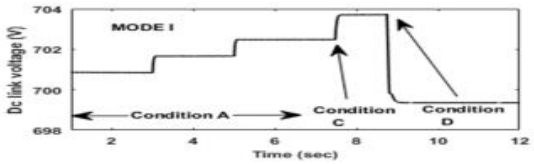

Fig. 17. DC link voltage variation

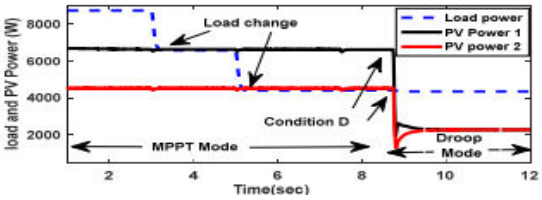

Fig. 18. PV1, PV2 and load powers.

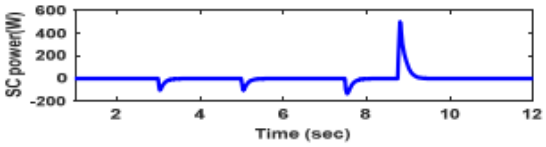

Fig. 19. Variations in SC power.

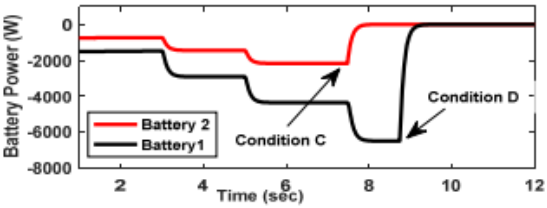

Fig. 20. Variations in BES powers.

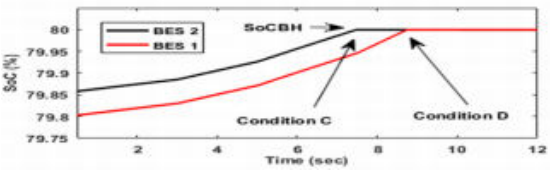

Fig. 21. Variations in % SoC BES

C. Experimental Results

The real time operation of the proposed MG1 with HES is implemented in FPGA platform which consist of Xilinx board programmed through National Instrument-PXIe chassis and analog signal acquisition by NI-PXIe 7853 R series channels. The proposed PMS is implemented in GUI based LABVIEW which provides switching pulses to all the converters and VSC. The hardware setup is presented in Fig. 22, consists of rooftop PV panels, 48 V lithium- ion battery, 32 V super capacitor pack, H-1000 Horizon PEM FC stack with its processor and dry H2 cylinder as well as boost and bidirectional converters. It also consists of 1 KVA Semikron inverter with LC filter. Ac bulb and dc Fan and light loads with controllable switch are used. The SC current reduces to 0.2 A to supply oscillatory power component in the MG, as shown in Fig. 23. Note, that the negative current direction of battery and SC shows discharging. Again at t2, the loads are switched ON.

Fig. 22. Experimental setup

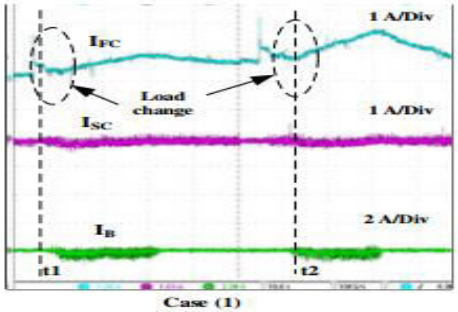

International Journal For Recent Developments in Science & Technology
2581-4575
Crossref
A Peer Reviewed Research Journal

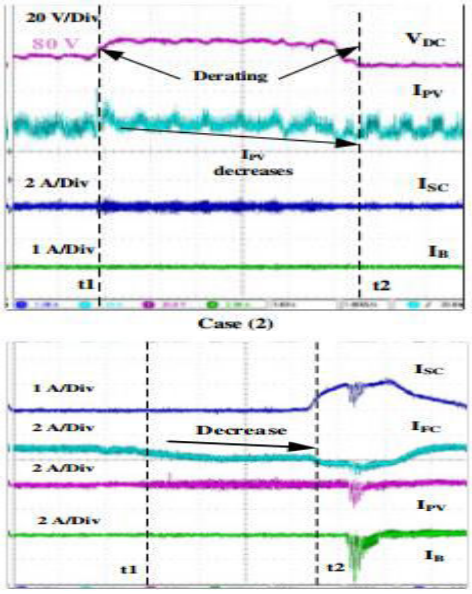

Fig. 23. Experimental results under various conditions.

The FC current ramps up from 0.6A and reaches 1 A in next 4s. The SC supplies transient 0.3A and then reduces to 0.2A. During this period, battery current increases from zero to 0.2A and then reduces to zero as FC reaches steady state. Thus, the PMS generates current references and PI based current controllers tracks them accurately. Case (2) refers to critical Condition E in mode I, which is consequent of Condition B, hence battery and FC current are zero initially. Since, PV power is more than load power and battery has already reached SoCBH hence, SC is charging to maintain the power balance. At instant t1, SC voltage reaches maximum voltage limit (VSCH). The SC current at instant t1 is 0.4 A while PV is supplying 1 A and dc link voltage is at reference of 80V. Now, the PV goes into de-rating mode with dc link voltage controller generating the duty ratio (D3) and subsequently operates PV at off MPPT. The PV current start decreasing at instant t1, dc link voltage rises slightly above to 82 V and at t2 the PV current reduces to 0.6 A, Isc reduces to zero and dc link voltage settles to 80 V reference. Thus, power balance is restored. Case (3), system works in Mode II Condition G. Initially at steady state, PV current is 0.2 A while FC supplies 2.5 A, battery supplies 0 A and SC supplies 0.2 A. Now, at instant t1, load is decreased so FC current decreases slowly to 2 A. At t2, the battery SoC reaches SoCBL. Hence, IB reduces to zero while dc link voltage is controlled by SC hence SC current increases to 0.8 A to maintain the power balance, as shown in Fig. 23.

5. CONCLUSION

The proposed PMS 1 for hybrid AC/DC MG1 successfully drives the MG1 from generation dominating mode to load dominating mode with efficient dc link voltage regulation. The presented PMS is robust to wide variation in operating point. The use of MAF efficiently separates the average current reference to be supplied by fuel cell and battery while transient and oscillatory component of power to be supplied by SC. The proposed MAF based multi-time scale adaptive droop PMS with supervisory control for MG2 offers reliable transition algorithm for operation of multiple PVs and BES in a geographically distributed location. It also considers the SoC charging and discharging rates for multiple BESs. Also, the PMS considers effective utilization of H2 in FC stack by using current slope limiter. The paper also proposes the control based PV power curtailment under critical conditions. The proposed PMS considers all the contingency conditions. The simulation and experimental results validates the proposed PMS under normal as well as critical conditions. Thus, PV-PEM fuel cell with HES and proposed PMS presents a promising scope for operation as a hybrid AC/DC microgrid

REFERENCES

[1] Lasseter R. H., “Micro-Grids”, in Proc.IEEE Power Engineering Society Winter Meeting, Vol. 1, pp. 305-308, 2002.

[2] Davis M. W., “Distributed resource electric power systems offer significant advantages over central station generation and T&D power

International Journal For Recent Developments in Science & Technology
2581-4575
Crossref
A Peer Reviewed Research Journal

systems, part I", IEEE T&D Conference and Exposition, Atlanta, Georgia, pp. 54-61, 2001.

[3] Lasseter R. H. and Piagi P., "MicroGrid: A conceptual solution", in Proc. Power Electronics Specialists Conference, Aachen, Germany, Vol. 6, pp. 4285-4290, 2001.

[4] Katiraei F. and Iravani M. R., "Transients of a Micro-Grid System with Multiple Distributed Energy Resources", International Conference on Power Systems Transients (IPST'05) in Montreal, Canada, June 19-23, 2005.

[5] Hajizadeh A. and Golkar M. A., "Intelligent Power Management Strategy of hybrid Distributed Generation System", Internationa Journal of Electrical Power and Energy Systems, Vol. 29, pp. 783-795, 2007.

[6] T. Ma, M. H. Cintuglu and O. A. Mohammed, "Control of a Hybrid AC/DC Microgrid Involving Energy Storage and Pulsed Loads," IEEE Transactions on Industry Applications, vol. 53, no. 1, pp. 567-575, Jan.- Feb. 2017.

[7] Xiong Liu, Peng Wang and P. C. Lon, "A hybrid AC/DC microgrid and its coordination control," IEEE Trans. Smart Grid, vol. 2, pp. 567-575, June. 2011.

[8] O.C. Onar, M. Uzunoglu and M. S. Alam, "Dynamic modelling, design and simulation of a wind/fuel cell/ultacapacitor based hybrid power generation system," Journal of Power Sources, vol. 161, pp. 707-722, Oct. 2006.

[9] M. Y. El-Sharkh et al, "A dynamic model for standalone fuel cell power plant for residential applications," Journal of Power Sources, vol. 138, pp. 199-204, Nov. 2004.

[10] S. Malo and R. Grino, "Design, Construction, and Control of a StandAlone Energy-Conditioning System for PEM-Type Fuel Cells," IEEE Transactions on Power Electronics, vol. 25, no. 10, pp. 2496-2506, Oct. 2010.

[11] Mahmud, M., Roy, T., Islam, S., Saha, S. and Haque, M. " Nonlinear Decentralized Feedback Linearizing Controller Design for Islanded DC Microgrids, " 2017 Electric Power Components and Systems, 45(16), pp.1747-176.

[12] R. K. Sharma and S. Mishra, "Dynamic Power Management and Control of a PV PEM Fuel-Cell-Based Standalone ac/dc Microgrid Using Hybrid Energy Storage," in IEEE Transactions on Industry Applications, vol. 54, no. 1, pp. 526-538, Jan.-Feb. 2018.

[13] M. B. Shadmand, R. S. Balog and H. Abu-Rub, "Model Predictive Control of PV Sources in a Smart DC Distribution System: Maximum Power Point Tracking and Droop Control," in IEEE Transactions on Energy Conversion, vol. 29, no. 4, pp. 913-921, Dec. 2014.

AUTHOR'S PROFILE:

[1]. G.S. BHANU SRI Pursuing her Masters Degree in Department of EEE from Kakinada Institute Of Technological Sciences (Kits), Ramachandrapuram.

[2]. DANDANGI RAMESH BABU , Completed his B.Tech Degree from Aditya Engineering College, Surampalem, Completed his M.Tech Degree from KITS Ramachandrapuram in EEE Department. Presently he is working as Assistant Professor in KITS Ramachandrapuram.. His Interested Area is Power Electronics.